Azimuth-elevation direction finding using a microphone and three orthogonal velocity sensors as a non-collocated subarray

Yang Song and Kainam Thomas Wong[a)]
Department of Electronic and Information Engineering, Hong Kong Polytechnic University, Hung Hom Kowloon KLN, Hong Kong

(Received 1 June 2012; revised 23 January 2013; accepted 25 January 2013)

An acoustic vector-sensor consists of three identical but orthogonally oriented acoustic particle-velocity sensors, plus a pressure sensor—all spatially **collocated** in a point-like geometry. At any point in space, this tri-axial acoustic vector-sensor can sample an acoustic wavefield as a 3×1 *vector*, instead of simply as a *scalar* of pressure. This *vector*, after proper self-normalization, would indicate the incident wave-field's propagation direction, and thus the incident emitter's azimuth-elevation direction-of-arrival. This "self-normalization" direction-of-arrival estimator is predicated on the spatial-*collocation* among the three particle-velocity sensors and the pressure-sensor. This collocation constriction is relaxed here by this presently proposed idea, to realize a *spatially distributed* acoustic vector-sensor, allowing its four component-sensors to be *separately* located. This proposed scheme not only retains the algorithmic advantages of the aforementioned "self-normalization" direction-of-arrival estimator, but also will significantly extend the spatial aperture to improve the direction-finding accuracy by orders of magnitude. © *2013 Acoustical Society of America*.
[http://dx.doi.org/10.1121/1.4792149]

PACS number(s): 43.30.Yj [ZHM] Pages: 1987–1995

I. INTRODUCTION

A. The acoustic particle-velocity sensor

Customary microphones (or hydrophones) treat the acoustic wavefield as a space-time field of pressure, which is a scalar at any specific time instant and any specific spatial location. Thereby overlooked is the underlying acoustic "particle-velocity vector"—a three-dimensional vector representing the pressure-field's three partial derivatives, taken with respect to the three Cartesian spatial coordinates. To physically measure any one such Cartesian component of this acoustic particle-velocity vector, needed is an acoustic particle-velocity sensor oriented along that Cartesian axis.

Acoustic particle-velocity sensor technology has been used in underwater-acoustics and air-acoustics for over a century,[1] and continues to draw interest.[2,3] The acoustic particle-velocity sensor's various hardware implementations are discussed in Ref. 4.

B. The customary acoustic *vector*-sensor: Three orthogonally oriented particle-velocity sensors collocating with a pressure sensor

The acoustic *vector*-sensor (i.e., vector-hydrophone), consists of three acoustic particle-velocity sensors (identical, collocated, but oriented orthogonally) plus an acoustic *pressure*-sensor—these four component-sensors together constitute one acoustic *vector*-sensor. Such an acoustic *vector*-sensor thereby distinctly measures each Cartesian component of the particle-velocity vector plus the pressure scalar, **all at the same point in three-dimensional space**.

Mathematically, for an acoustic *vector*-sensor located at the Cartesian coordinates' origin, it would have the 4×1 array-manifold[5–8]

$$\mathbf{a}(\theta, \phi) \stackrel{\text{def}}{=\!=} \begin{bmatrix} u(\theta, \phi) \\ v(\theta, \phi) \\ w(\theta) \\ 1 \end{bmatrix} \stackrel{\text{def}}{=\!=} \begin{bmatrix} \sin\theta\cos\phi \\ \sin\theta\sin\phi \\ \cos\theta \\ 1 \end{bmatrix} \tag{1}$$

in response to an incoming unit-power acoustic wave, that has traveled from the far field through an homogeneous isotropic medium. In the above, $\theta \in [0, \pi]$ symbolizes the elevation-angle measured from the positive z-axis, $\phi \in [0, 2\pi)$ denotes the azimuth-angle measured from the positive x-axis, and $u(\theta, \phi)$, $v(\theta, \phi)$, $w(\theta)$, respectively, refer to the direction-cosines along the x-, y-, and z-axis. The first, second, and third elements in $\mathbf{a}(\theta, \phi)$ each corresponds to an acoustic *velocity*-sensor aligned along the x-, y-, and z-axis, respectively. The array-manifold's fourth element corresponds to the acoustic *pressure*-sensor.

For a literature survey of the acoustic vector-sensor's hardware implementations, sea/air trials and associated direction-finding algorithms, please see Refs. 9–11. Air acoustic *vector*-sensors are commercially available as the "Ultimate Sound Probe" from Microflown Technologies in the Netherlands. Underwater acoustic *vector*-sensors are commercially available as the "Uniaxial P-U Probe" from Acoustech Corporation in the United States.

C. The acoustic *vector*-sensor's advantages in eigen-based direction-finding

The acoustic *vector*-sensor's unique array-manifold is advantageous to eigen-based direction-finding algorithms. It has been exploited using these various eigen-based

a)Author to whom correspondence should be addressed. Electronic mail: ktwong@ieee.org

parameter-estimation algorithms: "Estimation of Signal Parameters via a Rotation Invariance Technique" (ESPRIT), the Capon method, "Multiple Signal Classification" (MUSIC), Root-MUSIC, quaternion-MUSIC, beamspace-based DOA-estimation, or other subspace-based parameter-estimation methods. The acoustic *vector*-sensor has also been used for source-tracking. Please see Ref. 11 for a comprehensive literature review on such eigen-based direction-finding methods for the acoustic vector-sensor.

The above eigen-based algorithms eigen-decompose the space-time data-correlation matrix, to estimate each incident source's steering vector $\mathbf{a}$ as $\hat{\mathbf{a}} = c\mathbf{a}$, to within an unknown complex-value scalar c. Then, normalize $\hat{\mathbf{a}}$ to give $\sqrt{2}\hat{\mathbf{a}}/\|\hat{\mathbf{a}}\|$, of which the top three elements will be *un*ambiguous estimates of the three Cartesian direction-cosines $u(\theta, \phi)$, $v(\theta, \phi)$, and $w(\theta)$. Thereby, direction finding is thereby achieved, despite the unknown complex-value c mentioned above.

It is important to recognize that the above "self normalization" approach of direction-finding is predicated on a unity value for the fourth component regardless of the arrival-angles of θ and ϕ. This fact is used in the subsequently presented (4) and (14) to (16).

This acoustic *vector*-sensor "self-normalization" direction-finding is advantageous in the following ways.

{1} A four-component acoustic vector-sensor exploits information in the particle-velocity vector-field, in addition to the information in the pressure scalar field.
{2} Multiple incident sources' azimuth-angles and the elevation-angles may be estimated and automatically matched, using only one acoustic vector-sensor.[12]
{3} This self-normalization direction-finding approach may be creatively synergized with the customary interferometry direction-finding approach (which estimates the spatial phase delay among the data sets collected at physically displaced antennas) to offer unusual capabilities: (a) Direction-of-arrival improvement in estimation accuracy (under idealized scenarios) with*out* additional microphones/hydrophones;[13] (b) no prior knowledge/estimation is required of the nominal/actual geometric array-grid and no calibration-source is needed, for direction-of-arrival estimation;[14] and (c) no coarse estimate is *a priori* needed to initiate the iteration required by MUSIC. Instead, MUSIC becomes "self-initiating."[15]

D. This work's contributions

The direction-of-arrival estimation precision of a sensor-array depends on the spatial extent of the array aperture. The larger the aperture is, the finer the sensor-array's resolution will be for the direction-of-arrival. Unfortunately, the acoustic vector-sensor's spatial *collocation* gives a point-like aperture in space. While this spatial collocation simplifies the mathematics governing the acoustic vector-sensor's array manifold, thereby making possible the "self-normalization" approach of direction finding, it would be useful if the aperture may be enlarged without increasing the number of component-sensors, while retaining the full advantages of {1}–{3} above. Moreover, *hardware*-wise, it could be difficult and costly to physically collocate (or co-center) the four component-sensors all *exactly* at one point in space. This work will show how to displace the four component-sensors, while still retaining the aforementioned *algorithmic* advantages.

This contribution is nontrivial, as *spatially spread* particle-velocity sensors suffer phase-shifts among them, due to their displacements. Therefore, the array-manifold of (1) would become inapplicable, and the "self-normalization" direction-finding approach would apparently be inapplicable. Nonetheless, this paper succeeds in advancing a class of new closed-form direction-finding algorithms applicable even when the four component-sensors spread out arbitrarily in the three-dimensional space.

Besides retaining advantages {1}–{3} above, the presently proposed new class of algorithms *also* provide these additional advantages.

{4} The spatial resolution is enhanced over the azimuth/elevation, because the four component-sensors now extend over a larger spatial aperture (instead of co-centered at one point). That is, the present scheme spatially extends the geometric aperture, but requires *no* additional component-sensor.
{5} Hardware can be simplified, as the four component-sensors need no longer be collocated, thereby reducing the hardware cost.

The remainder of this paper is as follows: The new approach will be developed first for a simple array-geometry in Sec. II, as an illustrative case. For the general case of an *arbitrary* array-configuration of spatially spread particle-velocity sensors and pressure sensor, the new approach will be fully developed in Sec. III. Section IV will show how to adopt this new scheme to an eigen-based parameter-estimation algorithm, in the case of *one* acoustic vector-sensor, using[12] as a concrete example. Section V will do the same, but for the case of *multiple* acoustic vector-sensors, using[14] as a concrete example. Monte Carlo simulations there will verify the proposed scheme's efficacy in direction finding, despite

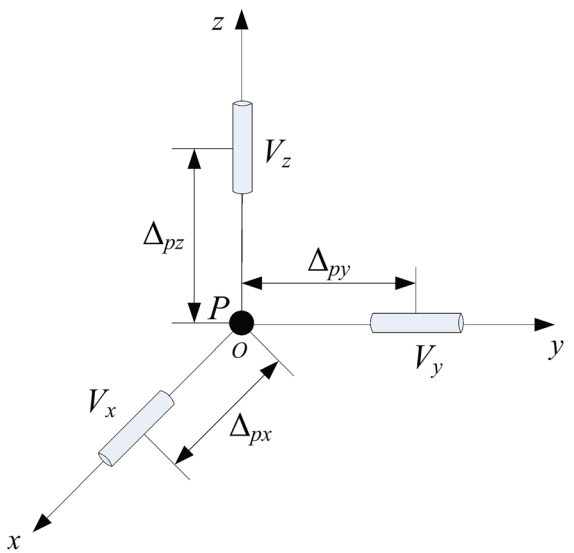

FIG. 1. (Color online) The "pyramid-like" array configuration with four component-sensors. Illustrated here is the special case of $\Delta_{px} > 0$, $\Delta_{py} > 0$, and $\Delta_{pz} > 0$.

the spatial non-collocation and the extended aperture of the acoustic vector-sensor. Section VI will conclude the paper.

II. THE NEW APPROACH—FOR A PARTICULARLY SIMPLE ARRAY CONFIGURATION, AS ILLUSTRATION

The proposed algorithmic approach allows all four component-sensors to be *arbitrarily located and arbitrarily oriented*. Nonetheless for pedagogical reasons, a particularly simple array-configuration (shown in Fig. 1) will first be discussed here in this section, to illustrate the proposed algorithmic philosophy. The arbitrarily general array-configuration will be discussed in details in Sec. III.

A. The array manifold for a particular array-configuration in Fig. 1

Referring to the sample array-configuration in Fig. 1: The pressure sensor lies at the Cartesian origin. The x-axis *oriented* particle-velocity sensor lies on the x-axis, at a distance of Δ_{px} from the Cartesian origin. The y-axis *oriented* particle-velocity sensor lies on the y-axis, at a distance of Δ_{py} from the Cartesian origin. The z-axis *oriented* particle-velocity sensor lies on the z-axis, at a distance of Δ_{pz} from the Cartesian origin. Here, Δ_{px}, Δ_{py}, or Δ_{pz} may each be positive or negative. Figure 1 illustrates one special case where $\Delta_{px}>0$, $\Delta_{py}>0$, and $\Delta_{pz}>0$. There in the figure, the particle-velocity sensors oriented along the x-axis, y-axis, and z-axis are identified, respectively, as V_x, V_y, and V_z, and the pressure sensor as P.

This *spatially distributed* array-configuration's array-manifold differs from the *spatially collocated* array-manifold in (1), but equals

$$\mathbf{a}_{\text{pyramid}}=\begin{bmatrix} ue^{j(2\pi/\lambda)\Delta_{px}u} \\ ve^{j(2\pi/\lambda)\Delta_{py}v} \\ we^{j(2\pi/\lambda)\Delta_{pz}w} \\ 1 \end{bmatrix}. \tag{2}$$

This new array-manifold in (2) now depends on the incident signal's frequency; and the Cartesian direction cosines now appear in the phases, in addition to the magnitudes in (1). The presence of $u(\theta, \phi)$, $v(\theta, \phi)$, $w(\theta)$ in the magnitudes (not in the phases) of this array manifold's entries allows unambiguous direction finding over the entire spherical surface spanned by $\theta \in [0, \pi]$ and $\phi \in [0, 2\pi)$, as will be shown in Sec. II B. This array configuration is "simple" relative to the more general arbitrarily spaced configuration to be introduced in Sec. III, in that the first three entries here in (2) each depends on only one of the three Cartesian direction cosines u, v, w.

B. A new direction-finding algorithm for a particular array-configuration in Fig. 1

Eigen-decompose the space-time correlation matrix of the data collected by the four component-sensors. Then obtainable, for each incident source, is the steering-vector estimate[16]

$$\hat{\mathbf{a}} \approx [p_x, p_y, p_z, p_p]^T \overset{\text{def}}{=\!=} c\,\mathbf{a}_{\text{pyramid}}, \tag{3}$$

where the superscript T denotes transposition. This steering-vector estimate $\hat{\mathbf{a}}$ is correct with regard to the true value $\mathbf{a}_{\text{pyramid}}$ to within an unknown complex-value constant c. With a noiseless condition or with an infinite number of snapshots, the above approximation becomes equality. To simplify the subsequent exposition, the following development will write all such approximations as equalities.

Normalize the first component of (3) by the fourth component, thereby giving

$$\frac{p_x}{p_p} = ue^{j(2\pi/\lambda)(\Delta_{px}u)}. \tag{4}$$

From (4), two complementary estimators of u are obtainable:

{1} An one-to-many relationship exists between $e^{j2\pi(\Delta_{px}/\lambda)u}$ and $u \in [-1, 1]$, for the extended aperture case of $(\Delta_{px}/\lambda) > (1/2)$. Hence,

$$\hat{u}_{\text{phs}} = \frac{1}{2\pi}\frac{\lambda}{\Delta_{px}}\angle\frac{p_x}{p_p} = m\frac{\lambda}{\Delta_{px}} + u \tag{5}$$

can estimate u, but ambiguously to within some (unknown) integer multiple $(m\times)$ of the frequency-*dependent* entity of $\pm(\lambda/\Delta_{px})$, where m refers to a to-be-determined integer.

{2} The frequency-*in*dependent entity

$$\hat{u}_{\text{mag}} = \left|\frac{p_x}{p_p}\right| = \pm u \tag{6}$$

can estimate u, but also ambiguously, to within a $\pm$ sign.

These two estimates, $\hat{u}_{\text{phs}}$ and $\hat{u}_{\text{mag}}$, can disambiguate each other as follows:

(a) If $\hat{u}_{\text{mag}} = u$, the cyclic ambiguity may be resolved by

$$\hat{m}_u^+ \overset{\text{def}}{=\!=} \underset{m}{\text{argmin}} \underbrace{\left|\left\{\left(m\frac{\lambda}{\Delta_{px}} + \overbrace{\frac{1}{2\pi}\frac{\lambda}{\Delta_{px}}\angle\frac{p_x}{p_p}}^{=\hat{u}_{\text{phs}}}\right) - \overbrace{\left|\frac{p_x}{p_p}\right|}^{=\hat{u}_{\text{mag}}}\right\}\right|}_{\overset{\text{def}}{=\!=}\epsilon_u^+(m)}. \tag{7}$$

(b) If $\hat{u}_{mag} = -u$, the cyclic ambiguity may then be resolved by

$$\hat{m}_u^- \overset{\text{def}}{=\!=} \underset{m}{\text{argmin}} \underbrace{\left|\left\{\left(m\frac{\lambda}{\Delta_{px}} + \overbrace{\frac{1}{2\pi}\frac{\lambda}{\Delta_{px}}\angle\frac{-p_x}{p_p}}^{=\hat{u}_{\text{phs}}}\right) - \overbrace{-\left|\frac{p_x}{p_p}\right|}^{=\hat{u}_{\text{mag}}}\right\}\right|}_{\overset{\text{def}}{=\!=}\epsilon_u^-(m)}. \tag{8}$$

(c) To decide between $\hat{u}_{\text{mag}} = u$ versus $\hat{u}_{mag} = -u$: Choose $\hat{u}_{\text{mag}} = u$, if if $\epsilon_u^+(\hat{m}_u^+) < \epsilon_u^-(\hat{m}_u^-)$. Choose $\hat{u}_{mag} = -u$, if $\epsilon_u^+(\hat{m}_u^+) \geq \epsilon_u^-(\hat{m}_u^-)$.

(d) Hence, u can now be *un*ambiguously estimated as

$$\hat{u} = \begin{cases} \left(\hat{m}_u^+ + \frac{1}{2\pi}\angle\frac{p_x}{p_p}\right)\frac{\lambda}{\Delta_{px}}, & \text{if} \quad \epsilon_u^+(\hat{m}_u^+) < \epsilon_u^-(\hat{m}_u^-) \\ \left(\hat{m}_u^- - \frac{1}{2\pi}\angle\frac{p_x}{p_p}\right)\frac{\lambda}{\Delta_{px}}, & \text{if} \quad \epsilon_u^+(\hat{m}_u^+) \geq \epsilon_u^-(\hat{m}_u^-). \end{cases} \tag{9}$$

The estimates, $\hat{v}$ and $\hat{w}$, may be obtained similarly as for $\hat{u}$ via Eqs. (4)–(9).

Finally, $\hat{u}$, $\hat{v}$, $\hat{w}$ together give the angle-of-arrival estimates,

$$\hat{\theta} = \arccos\hat{w}, \tag{10}$$

$$\hat{\phi} = \begin{cases} -\arccos\left[\frac{\hat{u}}{\sin(\hat{\theta})}\right], & \text{if} \quad \frac{\hat{v}}{\sin(\hat{\theta})} < 0 \\ \arccos\left[\frac{\hat{u}}{\sin(\hat{\theta})}\right], & \text{if} \quad \frac{\hat{v}}{\sin(\hat{\theta})} < 0. \end{cases} \tag{11}$$

This arrival-angle estimates enjoy a support-region over the entire spherical space spanning $\theta \in [0, \pi)$ and $\phi \in (-\pi, \pi]$. Hence, direction finding is achieved *un*ambiguously, despite the four component-sensors' non-collocation and despite their sparse spacings.

Because this "simple" array-configuration in (2) has its first three entries each dependent on only one of the three Cartesian direction cosines u, v, w, only one sign-ambiguity needs be disambiguated above for each velocity-sensor. In contrast, an arbitrarily spaced array-configuration (to be introduced in Sec. III) would be shown to require all three sign-ambiguities be handled for each velocity-sensor.

III. THE NEW SCHEME FOR THE GENERAL *ARBITRARY* ARRAY-CONFIGURATION

This section will show how the algorithmic philosophy in Sec. II can apply to the arbitrarily *general* array-configuration of Fig. 2.

A. The array manifold for the general array-configuration in Fig. 2

Let the pressure sensor be located again at the origin of the spherical coordinates, without loss of generality. However, allow the three orthogonally oriented particle-velocity sensors be placed *arbitrarily* in three-dimensional space.

For this general configuration of a spatially distributed acoustic vector-sensor, its 4×1 array-manifold equals

$$\mathbf{a}_{\text{gen}}(\theta,\phi) = \begin{bmatrix} u\, e^{j(2\pi/\lambda)[\Delta_{px}\sin\alpha_x\cos\beta_x u + \Delta_{px}\sin\alpha_x\sin\beta_x v + \Delta_{px}\cos\alpha_x w]} \\ v\, e^{j(2\pi/\lambda)[\Delta_{py}\sin\alpha_y\cos\beta_y u + \Delta_{py}\sin\alpha_y\sin\beta_y v + \Delta_{py}\cos\alpha_y w]} \\ w\, e^{j(2\pi/\lambda)[\Delta_{pz}\sin\alpha_z\cos\beta_z u + \Delta_{pz}\sin\alpha_z\sin\beta_z v + \Delta_{pz}\cos\alpha_z w]} \\ 1 \end{bmatrix}. \tag{12}$$

For the new symbols introduced in (13), please refer to Fig. 2 for their definitions.

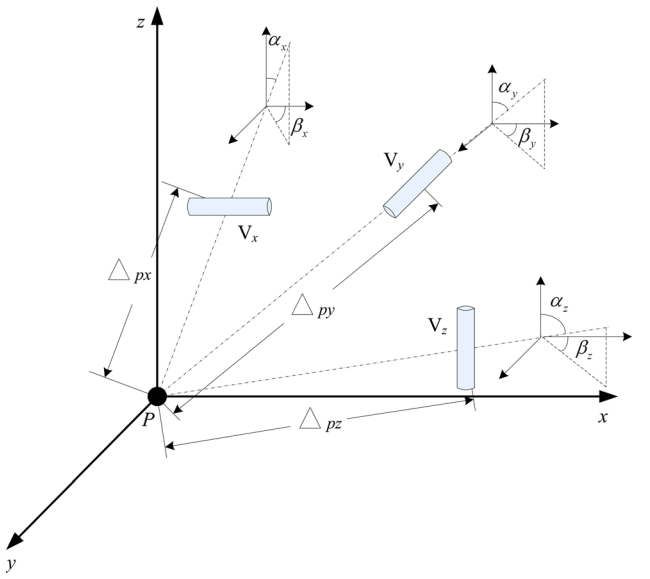

FIG. 2. (Color online) The acoustic vector-sensor's four component-sensors spaced arbitrarily in the three-dimensional space.

B. A new direction-finding algorithm for the general array-configuration in Fig. 2

Eigen-decompose the space-time data-correlation matrix of the data collected by the four component-sensors. Then, obtainable is the steering-vector estimate $\hat{\mathbf{a}}$ for each incident source, where

$$\hat{\mathbf{a}} \approx [p_x, p_y, p_z, p_p]^T \overset{\text{def}}{=\!=} c\,\mathbf{a}_{\text{gen}}. \tag{13}$$

Normalize each of the first three components of (13) by the fourth component, thereby producing

$$\frac{p_x}{p_p} = u\, e^{j(2\pi/\lambda)\Delta_{px}h_x}, \tag{14}$$

$$\frac{p_y}{p_p} = v\, e^{j(2\pi/\lambda)\Delta_{py}h_y}, \tag{15}$$

$$\frac{p_z}{p_p} = w\, e^{j(2\pi/\lambda)\Delta_{pz}h_z}, \tag{16}$$

where

$$h_x = u\sin(\alpha_x)\cos(\beta_x) + v\sin(\alpha_x)\sin(\beta_x) + w\cos(\alpha_x), \tag{17}$$

$$h_y = u\sin(\alpha_y)\cos(\beta_y) + v\sin(\alpha_y)\sin(\beta_y) + w\cos(\alpha_y), \tag{18}$$

$$h_z = u\sin(\alpha_z)\cos(\beta_z) + v\sin(\alpha_z)\sin(\beta_z) + w\cos(\alpha_z) \tag{19}$$

represent the direction-cosines obtained by projecting the propagation directional vector onto the axes on which Δ_{px}, Δ_{py}, Δ_{pz} lie, respectively. Please refer to Fig. 3. These non-Cartesian direction-cosines (h_x, h_y, h_z) are counterpart to the Cartesian direction-cosines (u, v, w) in the earlier Sec. II, where the three particle-velocity sensors are located on the three Cartesian axes.

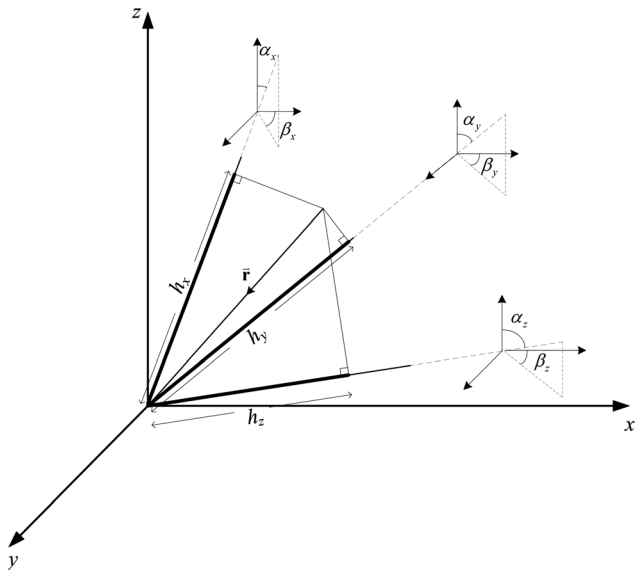

FIG. 3. A geometric illustration of h_x, h_y, and h_z.

The next Sec. III B 1 will explain how to estimate h_x, h_y, h_z, from which Sec. III B 2 will show how to estimate u, v, w.

1. Estimation of the non-Cartesian direction-cosines, h_x, h_y, h_z

Consider first the estimation of h_x.

From (14), two complementary estimators of h_x can be obtained (somewhat like the case in Sec. II):

(1) A many-to-one relationship exists between h_x and $e^{j2\pi(\Delta_{px}/\lambda)h_x}$, for a sparse spacing of $(\Delta_{px}/\lambda) > (1/2)$. In other words,

$$\hat{h}_{x,\text{phs}} = \frac{1}{2\pi}\frac{\lambda}{\Delta_{px}}\angle\frac{p_x}{p_p} = m\frac{\lambda}{\Delta_{px}} + h_x \tag{20}$$

would estimate h_x to ambiguously to within some integer multiple $(m\times)$ of the frequency-*dependent* entity of $\pm(\lambda/\Delta_{px})$, where m represents a to-be-determined integer.

(2) The magnitude $\hat{u}_{\text{mag}} = |p_x/p_p|, \hat{v}_{\text{mag}} = |p_y/p_p|$ and $\hat{w}_{\text{mag}} = |p_z/p_p|$ (all of which are frequency-*in*dependent) could estimate h_x to within a $\pm$ sign ambiguity. That is,

$$\hat{h}_{x,\text{mag}}^{(s_u,s_v,s_w)} = s_u\hat{u}_{\text{mag}}\sin(\alpha_x)\cos(\beta_x) + s_v\hat{v}_{\text{mag}}\sin(\alpha_x)\sin(\beta_x) + s_w\hat{w}_{\text{mag}}\cos(\alpha_x), \tag{21}$$

with $s_u, s_v, s_w \in \{+1, -1\}$.

Next, define

$$\hat{m}^{(s_u,s_v,s_w)} \overset{\text{def}}{=} \underset{m}{\text{argmin}} \underbrace{\left|\left\{\left[m\frac{\lambda}{\Delta_{px}} + \overbrace{\frac{1}{2\pi}\frac{\lambda}{\Delta_{px}}\angle\left(s_u\frac{p_x}{p_p}\right)}^{=\hat{h}_{x,\text{phs}}}\right] - \hat{h}_{x,\text{mag}}^{(s_u,s_v,s_w)}\right\}\right|}_{\overset{\text{def}}{=}\epsilon_x(m)}. \tag{22}$$

The sign ambiguity in each of s_u, s_v, s_w implies that there exist altogether eight possible candidates for $\hat{m}^{(s_u,s_v,s_w)}$.

The above procedure in (20)–(22) for h_x can be analogously applied for h_y and for h_z. To choose among the eight candidates of $\hat{m}^{(s_u,s_v,s_w)}$,[17] choose

$$(s_u^o, s_v^o, s_w^o) \overset{\text{def}}{=} \underset{(s_u,s_v,s_w)}{\arg\min} \sum_{\xi=x,y,z} \epsilon_\xi^2[\hat{m}^{(s_u,s_v,s_w)}]. \tag{23}$$

This allows h_x, h_y, and h_z to be *unambiguously* estimated as

$$\hat{h}_x = \left[\hat{m}^{(s_u^o,s_v^o,s_w^o)} + \frac{1}{2\pi}\angle\frac{s_u^o p_x}{p_p}\right]\frac{\lambda}{\Delta_{px}}, \tag{24}$$

$$\hat{h}_y = \left[\hat{m}^{(s_u^o,s_v^o,s_w^o)} + \frac{1}{2\pi}\angle\frac{s_v^o p_y}{p_p}\right]\frac{\lambda}{\Delta_{py}}, \tag{25}$$

$$\hat{h}_z = \left[\hat{m}^{(s_u^o,s_v^o,s_w^o)} + \frac{1}{2\pi}\angle\frac{s_w^o p_z}{p_p}\right]\frac{\lambda}{\Delta_{pz}}. \tag{26}$$

2. Estimation of the Cartesian direction-cosines u,v,w

To estimate the Cartesian direction-cosines u, v, w:

If $\text{r}(\mathbf{A}) = 3$ where $\text{r}(\cdot)$ denotes the rank of matrix,[18] then

$$\begin{bmatrix}\hat{u}\\ \hat{v}\\ \hat{w}\end{bmatrix} = \begin{bmatrix}\sin(\alpha_x)\cos(\beta_x) & \sin(\alpha_x)\sin(\beta_x) & \cos(\alpha_x)\\ \sin(\alpha_y)\cos(\beta_y) & \sin(\alpha_y)\sin(\beta_y) & \cos(\alpha_y)\\ \sin(\alpha_z)\cos(\beta_z) & \sin(\alpha_z)\sin(\beta_z) & \cos(\alpha_z)\end{bmatrix}^{-1} \times \begin{bmatrix}\hat{h}_x\\ \hat{h}_y\\ \hat{h}_z\end{bmatrix}. \tag{27}$$

The arrival-angles may thus be estimated as

$$\hat{\theta} = \arccos \hat{w}, \tag{28}$$

$$\hat{\phi} = \begin{cases} -\arccos\left[\dfrac{\hat{u}}{\sin(\hat{\theta})}\right], & \text{if } \dfrac{\hat{v}}{\sin(\hat{\theta})} < 0 \\ \arccos\left[\dfrac{\hat{u}}{\sin(\hat{\theta})}\right], & \text{if } \dfrac{\hat{v}}{\sin(\hat{\theta})} \geq 0. \end{cases} \tag{29}$$

Hence, a spatially spread acoustic vector-sensor can be used with *any* eigen-based parameter-estimation algorithm to perform direction finding. This technique may be applied to a *single* spatially spread acoustic vector-sensor alone (as will be demonstrated in Sec. IV), or to an array of *multiple* spatially spread acoustic vector-sensors (as will be demonstrated in Sec. V).

IV. A COMPLETE ALGORITHM TO DEMONSTRATE SEC. III'S PROPOSED SCHEME FOR A *SINGLE* ACOUSTIC VECTOR-SENSOR THAT IS SPATIALLY *DISTRIBUTED*

This section will demonstrate how the technique developed in Sec. III may be applied to a *single* spatially spread acoustic vector-sensor alone. This demonstration will be via adopting the "Uni-Vector-Hydrophone ESPRIT" algorithm of Ref. 12 (originally developed for an acoustic vector-sensor of *collocated* component-sensors) to accommodate a spatially *distributed* acoustic vector-sensor, via the technique in Sec. III.

A. A review of the Uni-Vector-Hydrophone ESPRIT algorithm, which is for one acoustic vector-sensor consisting of only collocated component-sensors

Suppose that K number of acoustic waves have traveled through an isotropic homogeneous medium, and impinge on an acoustic vector-sensor of spatially *collocated* component-sensors placed at the origin of the Cartesian coordinates. Suppose that the kth incoming signal $s_k(t)$ has power $\mathcal{P}_k$, a temporally monochromatic frequency f_k (which is distinct from all other incident signals' frequencies), and an initial phase φ_k.[19]

The 4×1 data-vector (observed at time t) equals

$$\mathbf{z}(t) = \sum_{k=1}^{K} \sqrt{\mathcal{P}_k}\mathbf{a}_k e^{j2\pi f_k t + \varphi_k} + \mathbf{n}(t), \tag{30}$$

where $\mathbf{a}_k = \mathbf{a}(\theta_k,\ \phi_k)$ symbolizes the kth incident source's steering vector from (1), and $\mathbf{n}(t)$ denotes the additive noise.

The *Uni-Vector-Hydrophone ESPRIT* algorithm[12] would form two time-delayed data-subsets, $\{\mathbf{z}(t_n), \forall n = 1, \ldots, N\}$ and $\{\mathbf{z}(t_n + \Delta_T), \forall n = 1, \ldots, N\}$, out of the observed data. In the above, Δ_T represents the time-delay between the two data-subsets.

The *Uni-Vector-Hydrophone ESPRIT* algorithmic steps are highlighted below. Their underlying motivations are explained in the detailed exposition in Ref. 12 itself.

{1} Form two $M \times N$ data-matrices $\mathbf{Z}_1 = [\mathbf{z}(t_1), \mathbf{z}(t_2), \ldots, \mathbf{z}(t_N)]$ and $\mathbf{Z}_2 = [\mathbf{z}(t_1 + \Delta_T), \mathbf{z}(t_2 + \Delta_T), \ldots, \mathbf{z}(t_N + \Delta_T)]$. Form a $2M \times N$ data-matrix $\mathbf{Z} = [\mathbf{Z}_1^T, \mathbf{Z}_2^T]^T$.

{2} Eigen-decompose $\mathbf{Z}\mathbf{Z}^H$ to give a $2M \times K$ signal-subspace eigenvector matrix $\mathbf{E}_s = [\mathbf{E}_1^T, \mathbf{E}_2^T]^T$, whose K columns contain the K principal eigenvectors corresponding to the K largest-magnitude eigenvalues.

{3} Compute a $K \times K$ matrix,

$$\mathbf{\Psi} \overset{\text{def}}{=\!=} (\mathbf{E}_1^H \mathbf{E}_1)^{-1}(\mathbf{E}_1^H \mathbf{E}_2) = \mathbf{T}^{-1}\mathbf{\Phi}\mathbf{T},$$

whose kth eigenvalue may be denoted as $\mathbf{\Psi}$ equals $[\mathbf{\Phi}]_{k,k} = e^{j2\pi f_k \Delta_T}$, with the kth column of $\mathbf{T}$ being the corresponding right-eigenvector, for all $k = 1, \ldots, K$.

{4} These K impinging sources' steering-vectors are estimated as

$$[\hat{\mathbf{a}}_1, \ldots, \hat{\mathbf{a}}_K] = \frac{1}{2}\{\mathbf{E}_1\mathbf{T}^{-1} + \mathbf{E}_2\mathbf{T}^{-1}\mathbf{\Phi}^{-1}\},$$

each to within an *unknown* complex-value multiplicative scalar, which arises from the eigen-decomposition of $\mathbf{\Psi}$.

{5} From $\hat{\mathbf{a}}_k$, the direction cosines may be estimated as

$$\hat{u}_k \overset{\text{def}}{=\!=} \frac{[\hat{\mathbf{a}}_k]_1}{[\hat{\mathbf{a}}_k]_4}, \tag{31}$$

$$\hat{v}_k \overset{\text{def}}{=\!=} \frac{[\hat{\mathbf{a}}_k]_2}{[\hat{\mathbf{a}}_k]_4}, \tag{32}$$

$$\hat{w}_k \overset{\text{def}}{=\!=} \frac{[\hat{\mathbf{a}}_k]_3}{[\hat{\mathbf{a}}_k]_4}, \tag{33}$$

where $[\mathbf{v}]_j$ symbolizes the jth entry of the vector $\mathbf{v}$. The kth source's two-dimensional direction-of-arrival may finally be estimated as

$$\hat{\theta}_k = \arcsin\left(\sqrt{\hat{u}_k^2 + \hat{v}_k^2}\right) = \arccos(\hat{w}_k), \tag{34}$$

$$\hat{\phi}_k = \arctan(\hat{v}_k / \hat{u}_k). \tag{35}$$

B. Applying Sec. III's proposed scheme to the Uni-Vector-Hydrophone ESPRIT algorithm for *one* acoustic vector-sensor with *spatially spread* component-sensors

Consider the spatially *spread* acoustic vector-sensor of Sec. III, instead of the spatially *collocated* acoustic vector-sensor in Ref. 12. The only change in the data-model of (30) is that now $\mathbf{a}_k = \mathbf{a}_{\text{gen}}(\theta_k,\ \phi_k)$ of (13). Then, Sec. IV A's algorithmic steps {1}–{4} remain valid with no change, step {5} of Sec. IV A now needs be replaced by the procedure in Sec. III.

Monte Carlo simulations below will demonstrate the proposed scheme's direction-finding efficacy and extended-aperture capability, despite the irregular array-configuration. The following settings are used for the array-configuration in Fig. 2: $\{\alpha_x = 80°,\ \beta_x = 15°\}$, $\{\alpha_y = 85°,\ \beta_y = 70°\}$, $\{\alpha_z = 10°,\ \beta_z = 40°\}$, $\Delta = \Delta_{px} = (20/7)\Delta_{py} = (20/9)\Delta_{pz}$. Two pure-tone signals at digital frequencies (i.e., the actual frequencies divided by the time-sampling frequency) $f_1' = 0.45$ and $f_2' = 0.3$, impinge, respectively, from $(\theta_1,\ \phi_1) = (60°,\ 140°)$

and $(\theta_2, \phi_2) = (125^\circ, -40^\circ)$. All incident signals have unity power. The complex-phases φ_1 and φ_2 are deterministic. The additive noise is zero-mean, Gaussian, white spatio-temporally, with a known power of $\sigma^2 = 20$ dB.

Figure 4(a) plots a composite root-mean-square-error (CRMSE)[20] of the first source's three Cartesian direction-cosine estimates, versus the inter-antenna spacing parameter Δ/λ, with λ referring to the shortest wavelength among all incident sources' wavelengths. Figure 4(b) does the same for the second source. This CRMSE is defined as $(1/I)\sum_{i=1}^{I}\sqrt{(\delta_{u,k,i}^2+\delta_{v,k,i}^2)/2}$, where $\delta_{u,k,i}$ ($\delta_{v,k,i}$) symbolizes the error in estimating the kth source's x-axis (y-axis) direction-cosine during the ith Monte Carlo experiment. Each data-point thereon consists of $I = 500$ statistically independent Monte Carlo experiments, each of which involves 200 temporal snapshots.

Figures 4(a) and 4(b) clearly demonstrate the proposed scheme's success in resolving the incident sources, even if the acoustic vector-sensor's four component-sensors are non-collocated and indeed very sparsely distributed in space. The collocated case (i.e., $\Delta = 0$) has its estimation error indicated in these figures by a dash-dot line, to ease comparison with the proposed scheme's performance. Note that the proposed scheme's estimation-error variance drops by about 1.5 orders-of-magnitude, as Δ increases (for the proposed scheme) by 2 orders-of-magnitude. Incidentally, this *ESPRIT*-based estimation approximates the Cramér-Rao lower bound, to the extent that *ESPRIT* does so.

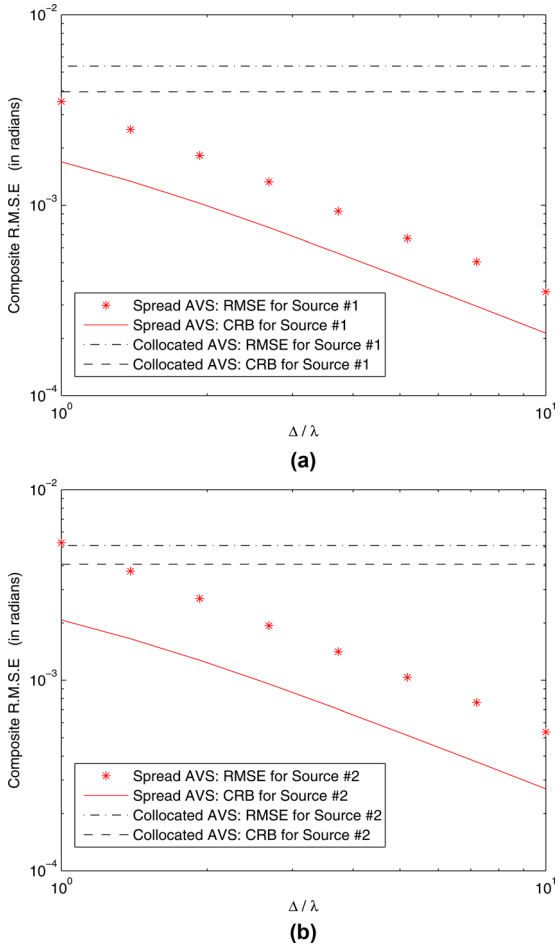

FIG. 4. (Color online) Monte Carlo simulations verifying the efficacy of the proposed scheme for a *single* acoustic vector-sensor alone.

V. A COMPLETE ALGORITHM TO DEMONSTRATE SEC. III's PROPOSED SCHEME FOR *SEVERAL* ACOUSTIC VECTOR-SENSORS, EACH OF WHICH IS SPATIALLY *DISTRIBUTED*

This section will demonstrate how the technique developed in Sec. III may be applied to a *several* spatially spread acoustic vector-sensors. This demonstration will be via adopting Wong and Zoltowski's algorithm of Ref. 14 (originally developed for acoustic vector-sensors each consisting of *collocated* component-sensors) to accommodate a spatially *distributed* acoustic vector-sensor, via the technique in Sec. III.

A. A review of Wong and Zoltowski's algorithm, which is for several acoustic vector-sensors each consisting of *collocated* component-sensors

Suppose that there exist L acoustic vector-sensors (with $L > K$) at arbitrary and possibly unknown locations. Let the lth acoustic vector-sensor's unknown location be (x_l, y_l, z_l). All else remains the same as in Sec. IV A.

The $4L \times 1$ array manifold for the entire L-element acoustic vector-sensor array is $\mathbf{a}_k \overset{\text{def}}{=} \mathbf{a}(\theta_k, \phi_k) \otimes \mathbf{q}(\theta_k, \phi_k)$, where the spatial phase factor $\mathbf{q}(\theta_k, \phi_k) \overset{\text{def}}{=} [e^{j2\pi(x_1 u_k + y_1 v_k + z_1 w_k)/\lambda_k}, \ldots, e^{j2\pi(x_L u_k + y_L v_k + z_L w_k)/\lambda_k}]^T$, and $\otimes$ symbolizes the Kronecker-product operator.

The $4L \times 1$ data-vector (observed at time t) equals

$$\mathbf{z}(t) = \sum_{k=1}^{K} \sqrt{\mathcal{P}_k}\mathbf{a}_k e^{j2\pi f_k t + \varphi_k} + \mathbf{n}(t). \tag{36}$$

Define a $4L \times K$ array matrix $\mathbf{A} \overset{\text{def}}{=} [\mathbf{a}_1, \ldots, \mathbf{a}_K]$ which may be partitioned into four $L \times 4$ subarray data blocks $\{\mathbf{A}_1, \ldots, \mathbf{A}_4\}$. $\mathbf{A}_j \overset{\text{def}}{=} \mathbf{J}_j\mathbf{A}$ and $\mathbf{J}_j \overset{\text{def}}{=} [\mathbf{0}_{L,L\times(j-1)}, \mathbf{I}_L, \mathbf{0}_{L,L\times(J-j),}]$ is a $L \times JL$ subarray-selection matrix, where $\mathbf{0}_{M,N}$ denotes a $M \times N$ zero matrix and $\mathbf{I}_M$ denotes an $M \times M$ identity matrix. Thus, the subarray data blocks $\{\mathbf{A}_1, \ldots, \mathbf{A}_4\}$ are interrelated as

$$\mathbf{A}_1 = \underbrace{\begin{bmatrix} u_1 & & \\ & \ddots & \\ & & u_K \end{bmatrix}}_{\overset{\text{def}}{=}\mathbf{\Phi}(u)} \mathbf{A}_4, \quad \mathbf{A}_2 = \underbrace{\begin{bmatrix} v_1 & & \\ & \ddots & \\ & & v_K \end{bmatrix}}_{\overset{\text{def}}{=}\mathbf{\Phi}(v)} \mathbf{A}_4,$$

$$\mathbf{A}_3 = \underbrace{\begin{bmatrix} w_1 & & \\ & \ddots & \\ & & w_K \end{bmatrix}}_{\overset{\text{def}}{=}\mathbf{\Phi}(w)} \mathbf{A}_4.$$

The algorithmic steps of Ref. 14 are highlighted below. Their underlying motivations are explained in the detailed exposition in Ref. 14 itself.

{1} Form two $M \times N$ data-matrices $\mathbf{Z} = [\mathbf{z}(t_1), \mathbf{z}(t_2), \ldots, \mathbf{z}(t_N)]$. Eigen-decompose $\mathbf{Z}\mathbf{Z}^H$ to give a $4L \times K$ signal-subspace eigenvector matrix $\mathbf{E}_s$, whose K columns contain the K principal eigenvectors corresponding to the K largest-magnitude eigenvalues.

{2} Construct the signal-subspace matrix pencil $\{\mathbf{E}_{s1}, \mathbf{E}_{s4}\}$, $\{\mathbf{E}_{s2}, \mathbf{E}_{s4}\}$, and $\{\mathbf{E}_{s3}, \mathbf{E}_{s4}\}$, where $\mathbf{E}_{s1} = \mathbf{J}_1\mathbf{E}_s$, $\mathbf{E}_{s2} = \mathbf{J}_2\mathbf{E}_s$, $\mathbf{E}_{s3} = \mathbf{J}_3\mathbf{E}_s$, and $\mathbf{E}_{s4} = \mathbf{J}_4\mathbf{E}_s$. Compute a $K \times K$ matrix,

$$\mathbf{\Psi}^{(u)} \stackrel{\text{def}}{=\!=} (\mathbf{E}_{s1}^H\mathbf{E}_{s1})^{-1}(\mathbf{E}_{s1}^H\mathbf{E}_{s4}) = [\mathbf{T}^{(u)}]^{-1}\mathbf{\Phi}^{(u)}\mathbf{T}^{(u)},$$

$$\mathbf{\Psi}^{(v)} \stackrel{\text{def}}{=\!=} (\mathbf{E}_{s2}^H\mathbf{E}_{s2})^{-1}(\mathbf{E}_{s2}^H\mathbf{E}_{s4}) = [\mathbf{T}^{(v)}]^{-1}\mathbf{\Phi}^{(v)}\mathbf{T}^{(v)},$$

$$\mathbf{\Psi}^{(w)} \stackrel{\text{def}}{=\!=} (\mathbf{E}_{s3}^H\mathbf{E}_{s3})^{-1}(\mathbf{E}_{s3}^H\mathbf{E}_{s4}) = [\mathbf{T}^{(w)}]^{-1}\mathbf{\Phi}^{(w)}\mathbf{T}^{(w)},$$

where $\mathbf{T}^{(u)}$, $\mathbf{T}^{(v)}$, and $\mathbf{T}^{(w)}$ are nonsingular matrices.

{3} These K impinging sources' steering-vectors are estimated as

$$[\hat{\mathbf{a}}_k]_1 \approx [\mathbf{\Phi}^{(u)}]_{k,k},$$

$$[\hat{\mathbf{a}}_k]_2 \approx [\mathbf{\Phi}^{(v)}]_{k,k},$$

$$[\hat{\mathbf{a}}_k]_3 \approx [\mathbf{\Phi}^{(w)}]_{k,k},$$

for $k = 1, \ldots, K$, where $[\mathbf{M}]_{i,j}$ symbolizes the (i, j)th entry of the matrix $\mathbf{M}$.

{4} From $\hat{\mathbf{a}}_k$, the direction cosines may be estimated as

$$\hat{u}_k \stackrel{\text{def}}{=\!=} [\hat{\mathbf{a}}_k]_1, \tag{37}$$

$$\hat{v}_k \stackrel{\text{def}}{=\!=} [\hat{\mathbf{a}}_k]_2, \tag{38}$$

$$\hat{w}_k \stackrel{\text{def}}{=\!=} [\hat{\mathbf{a}}_k]_3. \tag{39}$$

The kth source's two-dimensional direction-of-arrival may finally be estimated as

$$\hat{\theta}_k = \arcsin\left(\sqrt{\hat{u}_k^2 + \hat{v}_k^2}\right) = \arccos(\hat{w}_k), \tag{40}$$

$$\hat{\phi}_k = \arctan(\hat{v}_k/\hat{u}_k). \tag{41}$$

B. Applying Sec. III's proposed scheme to Wong and Zoltowski's algorithm for *multiple* acoustic vector-sensors each with *spatially spread* component-sensors

Consider an array of several spatially *spread* acoustic vector-sensor, instead of the spatially *collocated* acoustic vector-sensor in Ref. 14. The only change in the data-model of (36) is that now $\mathbf{a}_k = \mathbf{a}_{\text{gen}}(\theta_k, \phi_k) \otimes \mathbf{q}(\theta_k, \phi_k)$. Then, Sec. V A's algorithmic steps {1}–{3} remain valid with no change, step {4} of Sec. V A now needs be replaced by the procedure in Sec. III. Monte Carlo simulations below will verify the efficacy of this synergy.

Here, $L = 5$, at the locations of $(3.9\lambda, 2.1\lambda, 1.8\lambda)$, $(2.1\lambda, 0.9\lambda, 1.5\lambda)$, $(4.5\lambda, 3.6\lambda, 5.7\lambda)$, $(2.1\lambda, 3.3\lambda, 1.5\lambda)$, $(6.0\lambda, 5.4\lambda, 3.3\lambda)$. Each acoustic vector-sensor follows the spatial distribution array-configuration in Fig. 2, with $\{\alpha_x = 15°, \beta_x = 75°\}$, $\{\alpha_y = 40°, \beta_y = 45°\}$, $\{\alpha_z = 35°, \beta_z = 85°\}$, $\Delta = \Delta_{px} = (20/7)\Delta_{py} = (20/9)\Delta_{pz}$.

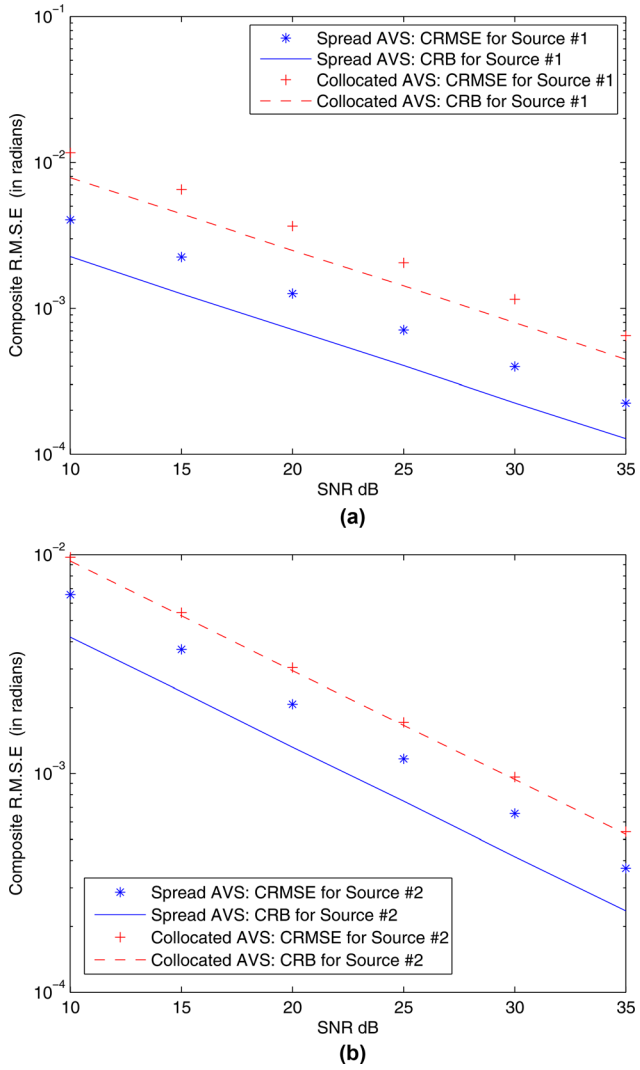

FIG. 5. (Color online) Monte Carlo simulations verifying the efficacy of the proposed scheme for *multiple* acoustic vector-sensors.

Two pure-tone signals at digital frequencies $f_1' = 0.4$ and $f_2' = 0.3$, impinge, respectively, from $(\theta_1, \phi_1) = (60°, 135°)$ and $(\theta_2, \phi_2) = (150°, -40°)$. All incident signals have unity power. The complex-phases φ_1 and φ_2 are deterministic.

Figure 5(a) plots a CRMSE of the first source's three Cartesian direction-cosine estimates, versus the signal-to-noise ratio SNR when $\Delta/\lambda = 3$. Figure 5(b) does the same for the second source. Each data-point thereon consists of $I = 500$ statistically independent Monte Carlo experiments, each of which involves 100 snapshots. Noticeably lower estimation errors are offered by the spatially spread constitution of each acoustic vector-sensor, relative to the case of collocated component-sensors within each acoustic vector-sensor.

VI. CONCLUSION

Many advantages are advanced by the recent synergy between customary interferometry-based direction finding and the new self-normalization approach of direction finding. This paper further generalizes this synergy, by proposing a

new direction-finding algorithm to allow the acoustic vector-sensor's four component-sensors may be spatially displaced over a general array-grid, perhaps with a much extended spatial aperture, thereby improving direction-finding accuracy by *orders of magnitude*, while mitigating hardware-implementation difficulties in spatially collocating the four component-sensors at one point in space.

An electromagnetic counterpart exists in Ref. 21 for this proposed acoustic vector-sensor scheme. Both the electromagnetic and the acoustic schemes are predicated on how each component-sensor's magnitude relates to the incident sources' unknown but to-be-estimated parameters. Due to the fundamental differences between acoustics and electromagnetics, these magnitudes take on entirely different mathematical forms. Hence, the proposed algorithmic steps (and the applicable array configurations) are fundamentally different here from.[21]

ACKNOWLEDGMENT

This work was supported by the Hong Kong Polytechnic University's Internal Competitive Research Grant #G-YG67.

[1]C. B. Leslie, J. M. Kendall, and J. L. Jones, "Hydrophone for measuring particle velocity," J. Acoust. Soc. Am. **28**, 711–715 (1956).
[2]M. J. Berliner and J. F. Lindberg, *Acoustical Particle Velocity Sensors: Design, Performance and Applications* (AIP Press, Woodbury, NY, 1996), pp. 1–448.
[3]V. A. Shchurov, *Vector Acoustics of the Ocean* (Dalnauka, Vladivostok, Russia, 2006), pp. 1–297.
[4]K. T. Wong and H. Chi, "Beam patterns of an underwater acoustic vector hydrophone located away from any reflecting boundary," IEEE J. Oceanic Eng. **27**, 628–637 (2002).
[5]A. Nehorai and E. Paldi, "Acoustic vector-sensor array processing," IEEE Trans. Signal Process. **42**, 2481–2491 (1994).
[6]B. A. Cray and A. H. Nuttall, "Directivity factors for linear arrays of velocity sensors," J. Acoust. Soc. Am. **110**, 324–331 (2001).
[7]J. A. McConnell, "Analysis of a compliantly suspended acoustic velocity sensor," J. Acoust. Soc. Am. **113**, 1395–1405 (2003).
[8]Y. I. Wu, K. T. Wong, and S.-K. Lau, "The acoustic vector-sensor's near-field array-manifold," IEEE Trans. Signal Process. **58**, 3946–3951 (2010).
[9]P. K. Tam and K. T. Wong, "Cramer-Rao bounds for direction finding by an acoustic vector sensor under nonideal gain-phase responses, noncollocation, or nonorthogonal orientation," IEEE Sensors J. **9**, 969–982 (2009).
[10]K. T. Wong, "Acoustic vector-sensor 'blind' beamforming and geolocation for FFH-sources," IEEE Trans. Aerosp. Electron. Syst. **46**, 444–448 (2010).
[11]Y. I. Wu and K. T. Wong, "Acoustic near-field source-localization by two passive anchor-nodes," IEEE Trans. Aerosp. Electron. Syst. **48**, 159–169 (2012).
[12]P. Tichavsky, K. T. Wong, and M. D. Zoltowski, "Near-field/far-field azimuth and elevation angle estimation using a single vector hydrophone," IEEE Trans. Signal Process. **49**, 2498–2510 (2001).
[13]K. T. Wong and M. D. Zoltowski, "Extended-aperture underwater acoustic multi-source azimuth/elevation direction-finding using uniformly but sparsely spaced vector hydrophones," IEEE J. Oceanic Eng. **22**, 659–672 (1997).
[14]K. T. Wong and M. D. Zoltowski, "Closed-form underwater acoustic direction-finding with arbitrarily spaced vector hydrophones at unknown locations," IEEE J. Oceanic Eng. **22**, 649–658 (1997).
[15]K. T. Wong and M. D. Zoltowski, "Self-initiating music-based direction finding in underwater acoustic particle velocity-field beamspace" IEEE J. Oceanic Eng. **25**, 262–273 (2000).
[16]This would not limit this proposed scheme to only one incident source.
[17]The above number of candidates may be reduced, if prior knowledge exists of the specific hemisphere or quadrant from which the incident source impinges. For example, suppose a source is prior known to impinge from the upper hemisphere: Then $w>0$, i.e., $s_{x,w}=s_{y,w}=s_{z,w}=+1$, thereby $s_w^o=+1$. The number of possible candidates in (22) and (23) would then reduce from eight to four. Only $\{s_u^o, s_v^o\}$ needs to be determined in step (b).
[18]The following square matrix is invertible, iff $(\alpha_\xi, \beta_\xi) \neq (\alpha_\nu, \beta_\nu)$ and $(\alpha_\xi, \beta_\xi) \neq (\pi - \alpha_\nu, \beta_\nu \pm \pi), \forall \xi \neq \nu$ where $\xi, \nu \in \{x, y, z\}$. In terms of the array-configuration in Fig. 2, this represents a mild condition that no two particle-velocity sensors may lie on a same radial line emanating from the Cartesian coordinates' origin.
[19]The technique proposed in Sec. III may be readily applied to other data models and is not restricted to the one reviewed here of Ref. 12. This present data model serves only as an illustrative example. For example, wideband signals could be handled, by first applying the short-time discrete Fourier transform (DFT) to the time-domain data, then each DFT-component can be subsequently processed individually.
[20]The estimation bias is about an order-of-magnitude smaller than the corresponding estimation standard deviation, and hence not shown.
[21]K. T. Wong and X. Yuan, "Vector cross-product direction-finding with an electromagnetic vector-sensor of six orthogonally oriented but spatially noncollocating dipoles/loops," IEEE Trans. Signal Process. **59**, 160–171 (2011).